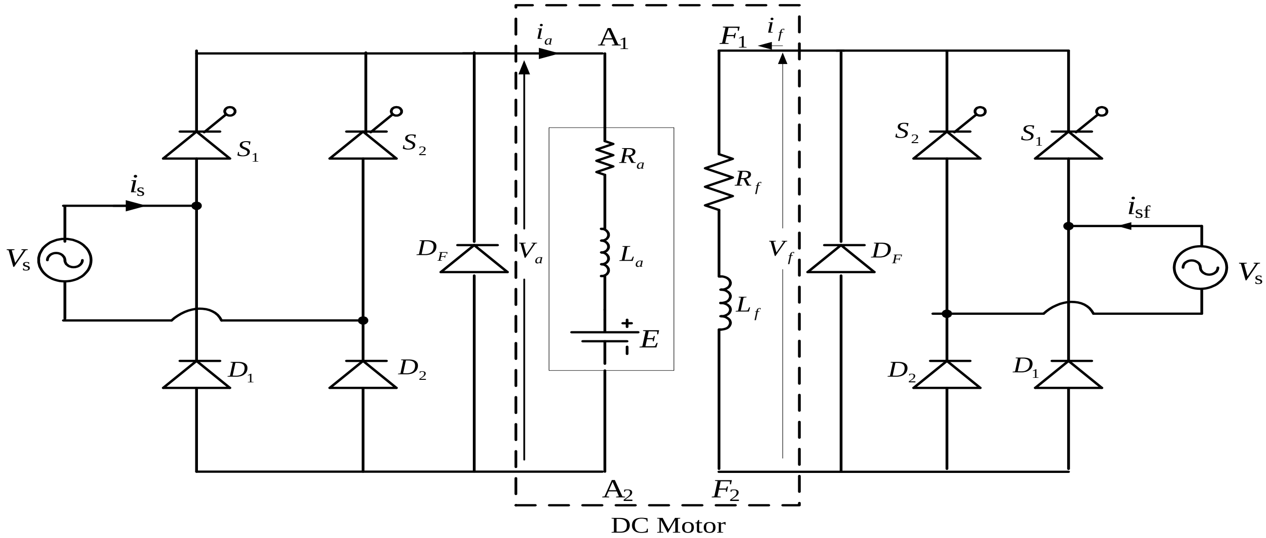

Fig. 5: Circuit of Single-phase Semi-Converter-Controlled DC Motor

During the positive half-cycle, thyristor T_1 is forward biased. When thyristor T_1 is fired at $\omega t = \alpha,$ the load is connected to the input supply through T_1 and D_2 during the period $\propto \leq \ \omega t \ \leq \pi$. During the period $\pi \ \leq \ \omega t \ \leq (\pi + \propto)$, the input voltage is negative and the freewheeling diode D_m is forward biased. D_m provides continuity of current in the inductive load. The load current is transferred from T_1 and D_2 to D_m; and thyristor T_1 and diode D_2 are turned off. During the negative half-cycle of input voltage, thyristor T_2 is forward biased, and firing of thyristor T_2 at $\omega t = \pi + \alpha$ will reverse bias D_m. The diode D_m is turned off and the load is connected to the supply through T_2 and D_1.

$$V_o = \frac{1}{2\pi}\int_0^{2\pi} V_m \sin\omega t d\omega t = \frac{V_m}{2\pi}\left\{\int_\alpha^\pi \sin\omega t d\omega t - \int_{\pi+\alpha}^{2\pi} \sin\omega t d\omega t\right\} = \frac{V_m}{\pi}\left(1+\cos\alpha\right) \tag{25}$$

The average load current then becomes:

$$I_o = \frac{V_o - E}{R} \tag{26}$$

The output voltage v_o can be expressed in Fourier series as:

$$v_o = V_o + \sum_{n=1}^{\infty}\left(a_n \cos n\omega t + b_n \sin n\omega t\right) \tag{27}$$

Where

$$a_n = \frac{V_m}{\pi}\left\{\int_\alpha^\pi \sin\omega t \cos n\omega t \, d\omega t + \int_{\pi+\alpha}^{2\pi} \sin\omega t \cos n\omega t \, d\omega t\right\} \tag{28}$$

$$b_n = \frac{1}{\pi}\left\{\int_{\alpha}^{\pi} V_m \sin\omega t \sin n\omega t \, d\omega t + \int_{\pi+\alpha}^{2\pi} V_m \sin\omega t \sin n\omega t \, d\omega t\right\} \tag{29}$$

$$i_o = \sum_{n=1}^{\infty} \frac{1}{Z_n}\left[a_n \cos(n\omega t - \theta_n) + b_n \sin(n\omega t - \theta_n)\right] \tag{30}$$

$$Z_n = \sqrt{R^2 + (n\omega L)^2} \;\; ; \;\; \theta_n = \tan^{-1}\left(\frac{n\omega L}{R}\right)$$

Under steady-state conditions, the armature voltage is:

$$V_a = \frac{V_m}{\pi}(1 + \cos\alpha) \tag{31}$$

The Field circuit voltage is:

$$V_f = \frac{V_m}{\pi}(1 + \cos\alpha_f) \tag{32}$$

From the dc motor operating equations derived earlier, the following equations are produced in conjunction with the rectifier output voltage:

$$I_a = \frac{V_a - E}{R_a} = \frac{V_a - k I_f \omega_m}{R_a} \tag{33}$$

$$I_f = \frac{V_f}{R_f} \tag{34}$$

$$T_a = k I_f I_a = K I_a \tag{35}$$

$$\omega_m = \frac{V_a - I_a R_a}{K} \tag{36}$$

$$\omega_m = \frac{V_a}{K} - \frac{R_a}{(K)^2} T_a \tag{37}$$

III. RESULTS AND DISCUSSIONS

The control equations derived in chapter three of this thesis are plotted here, where,

$P = 1500$ W, $V_a = 200$ V, $I_a = 15$ A, $N_m = 1500$ rpm, $R_a = 6.5\,\Omega$, $L_a = 25$ mH, $R_f = 100\,\Omega$, Source voltage, $V_s = 230$ V, $f = 50$ Hz, $J = 0.1$ kg-m^2, $B = 0.038$ N.m/rad/s.

The armature voltage required to drive the motor at rated speed (157 rad/s) is 200 V, as expressed in equation (23). The plot is shown in Figure 6. Figure 6 is the time response of the motor speed due to step change in the armature voltage.

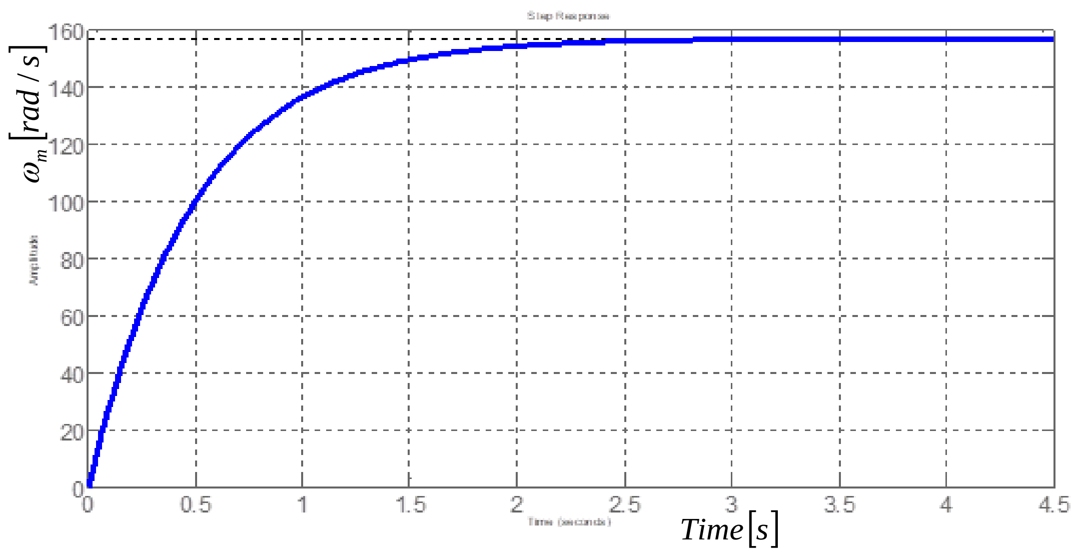

Fig 6 Speed response due to step change in armature voltage.

Application of the rated load of 9.55 N.m, at rated armature voltage of 200 V reduces the motor speed to 110 rad/s as shown in Figure 7 and expressed by equation (24). Figure 7 is the time response of the motor speed due to step change in the load torque. This is the full-load speed.

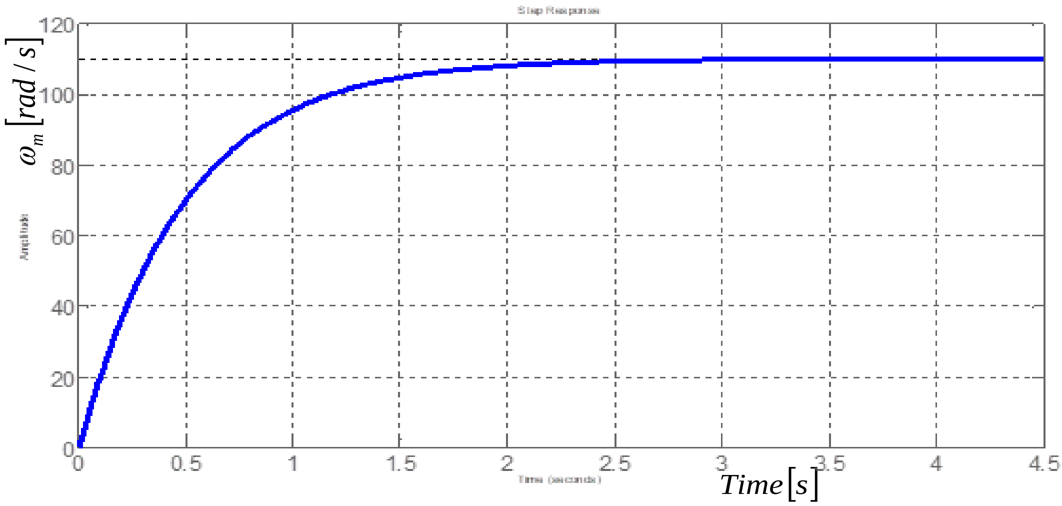

Fig.7 Speed response due to step change in armature voltage and load torque.

The output voltage and output current of the rectifier are expressed in Equations (25), (26), (27) and (30). They are ploted against time as shown in Figure 8. v_o and i_o are the instantaneous quantities, while V_o and I_o are the average values. It can be noticed in Figure 8 that $V_o = 200\,\text{V}$, $I_o = 15\,\text{A}$, the rated values of the motor, where $\alpha = 21.3^o$.

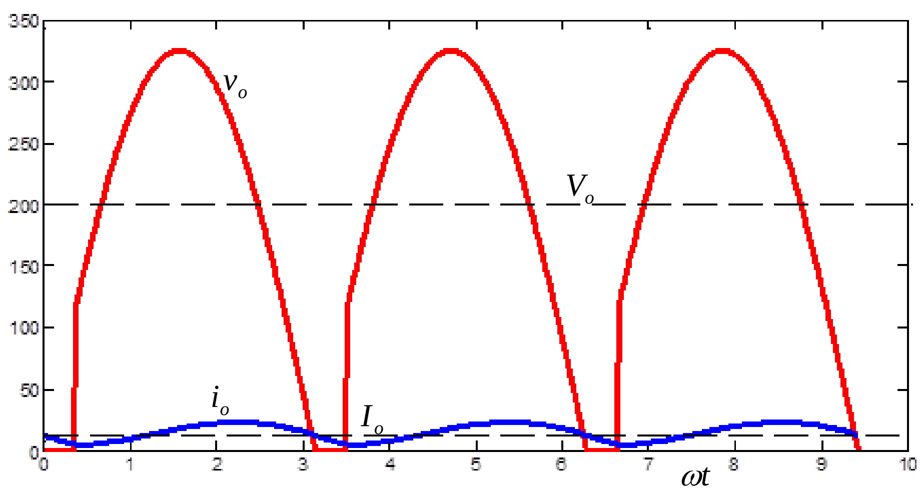

Fig. 8: Output Voltage and Current Waveforms of the armature circuit rectifier

Equation (31) is plotted as shown in Figure 9 which shows how the rectifier output voltage (V_a) varies with the delay angle (α). α is adjustable between 0^o and 90^o. The maximum armature voltage obtainable is 207 V, at $\alpha = 0^o$. At the delay angle of 90º, $V_a = 103\,\text{V}$. At $\alpha = 21.3^o$, the rated voltage of the motor, 200 V is applied across the armature.

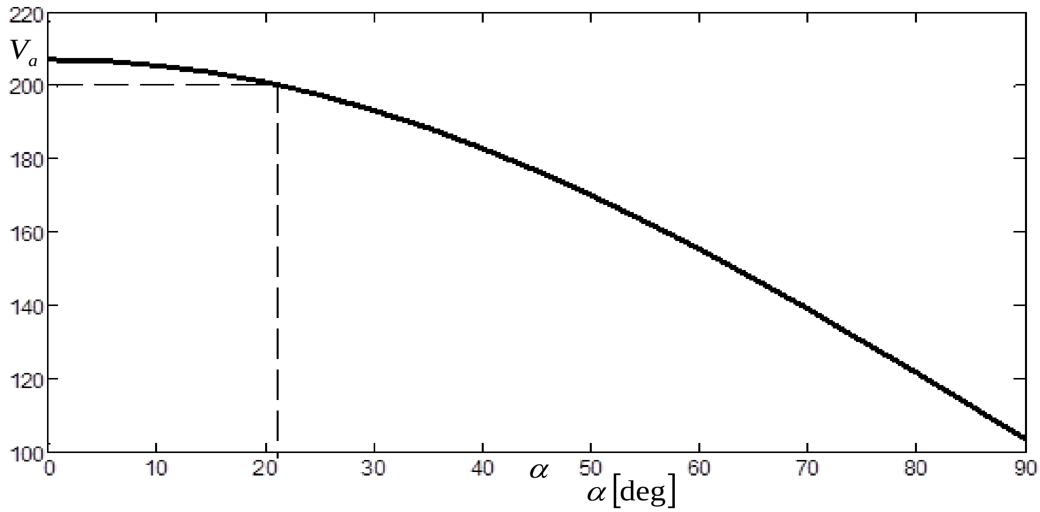

Fig. 9 Variation of armature voltage V_a with delay angle α

Equation (35) shows that the developed torque is directly proportional to the armature current. This is shown in Figure 10. The speed of dc motor changes with the load torque. To maintain a constant speed, the armature voltage or field voltage should be varied continuously by varying the delay angle of ac-dc converters. Thus, an increase in voltage will result in a proportional increase in current, and consequently an increase in developed torque as shown in Figure 10. The figure shows that the torque of 15.52 N.m is developed at the rated current and rated voltage of 15 A and 200 V respectively

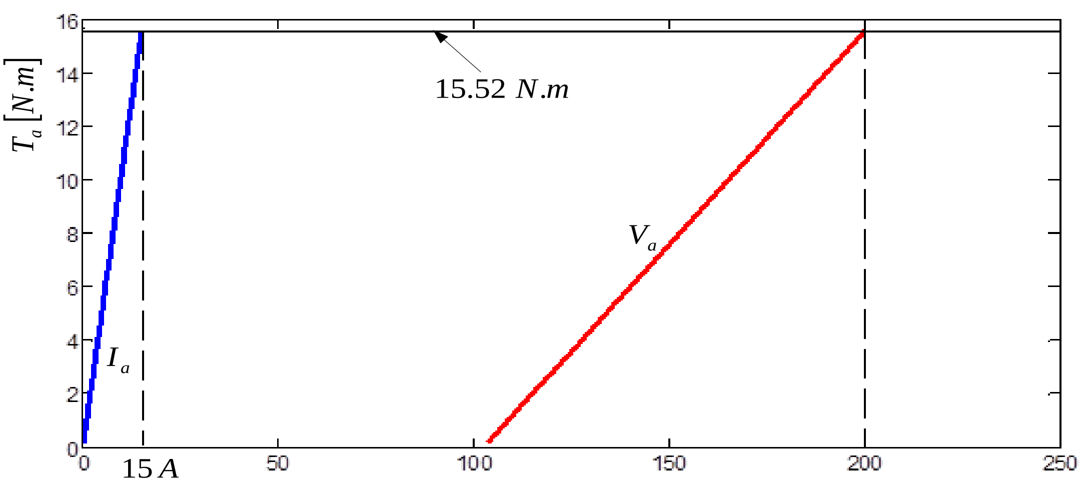

.Fig. 10 Plot of developed torque ((T_m) versus armature voltage (V_a) and armature current (I_a)

Equation (36) shows that if the armature current increases proportionally with increase in the armature voltage, the speed remains constant, as shown in Figure 11, and since the current is increasing, the developed torque also increases in accordance with equation (3.45).

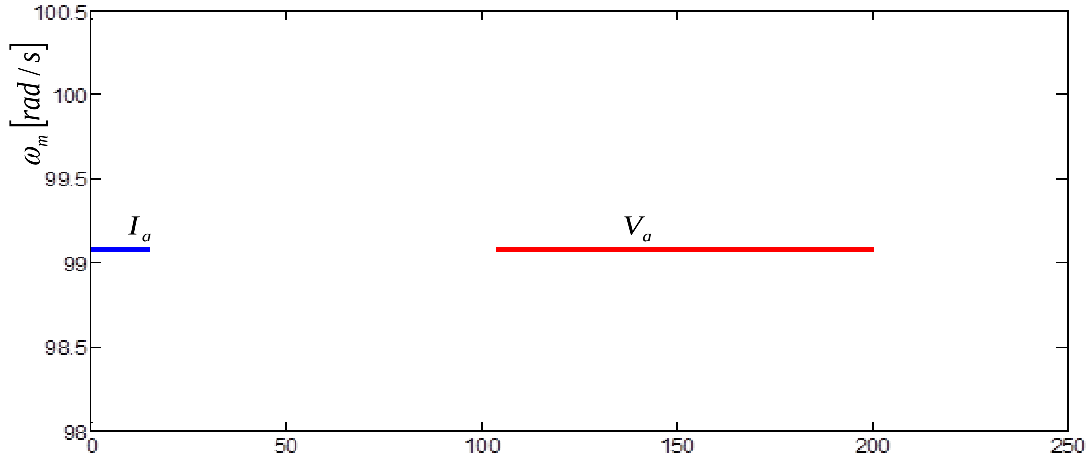

Fig. 11: Plot of motor speed versus armature voltage and current

In equation (37), the torque is kept constant at rated value, while the armature voltage is varied to control the speed. Figure 12 shows how the speed (ω_m) of the motor varies with the armature voltage (V_a). The speed increases as the armature voltage increases.

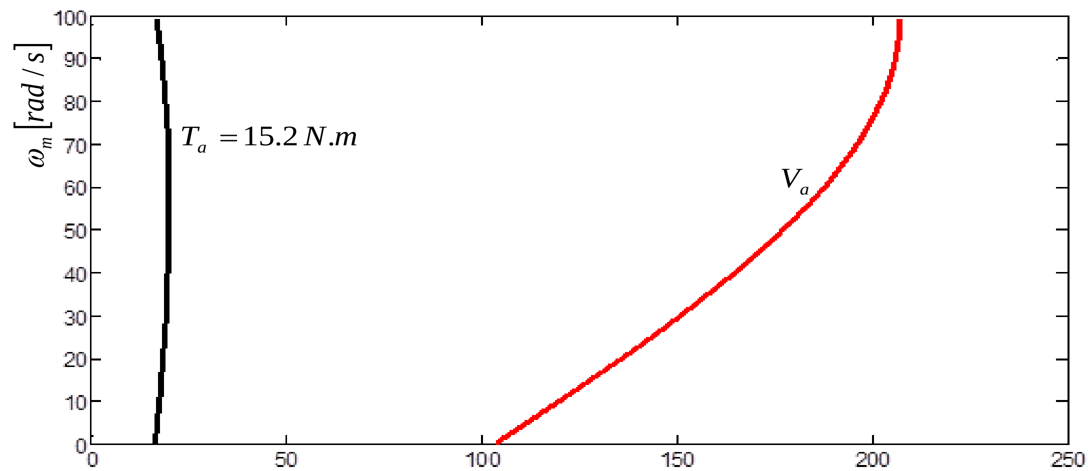

Fig. 12: Speed (ω_m) versus armature voltage (V_a) and developed torque $(\mathrm{T_a})$

When the motor is to run above base speed, field control is applied The base speed is the speed obtained at the rated armature voltage. Speed is increased by decreasing the field voltage, while the armature voltage is maintained constant at rated value. Decreasing V_f leads to decrease in I_f. Figure 13 shows the variation of speed with the field excitation. It can be observed that the speed (ω_m) is inversely proportional to the field current (I_f), as indicated in equation (36). The speed is increased by decreasing the field current (I_f).

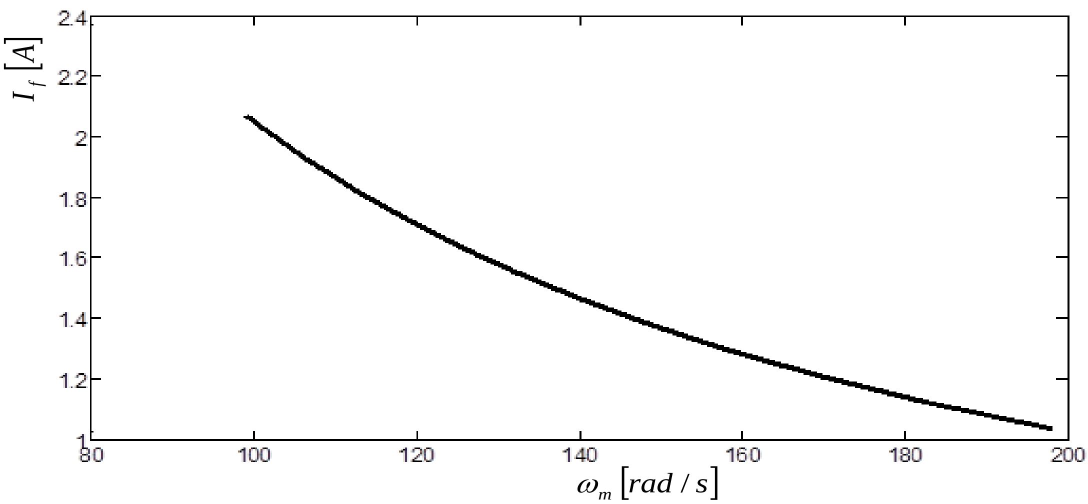

Fig. 13: Plot of speed versus field current

Figure 14 is the plot of torque versus field current. It shows that the developed torque (T_a) increases with increase in field current (I_f), as expressed in equation (35).

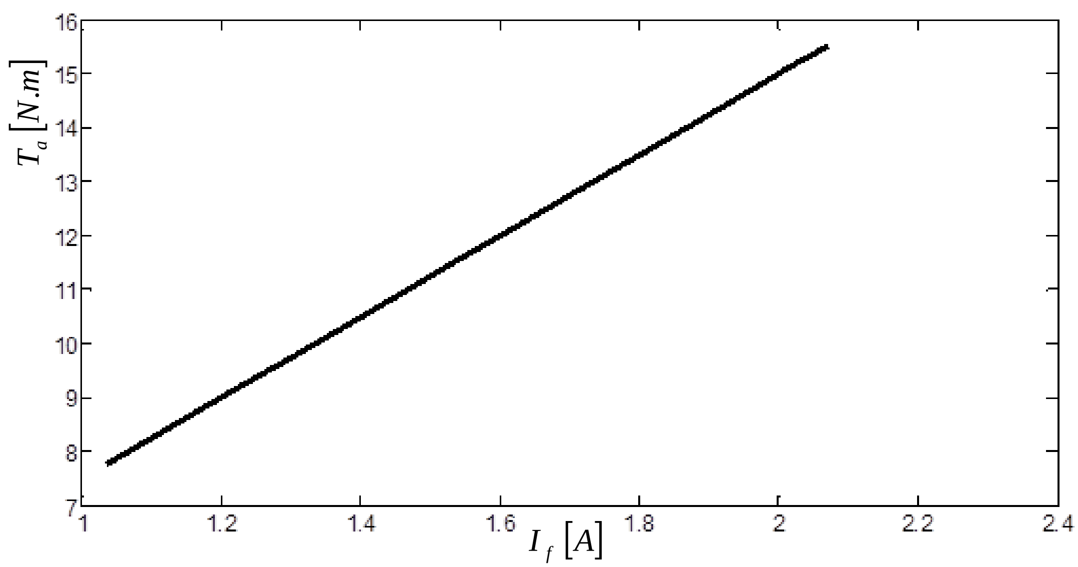

Fig. **1**4: Plot of Torque Versus Field Current

The speed-torque characteristic of the motor is shown in Figure 15. It shows that the speed (ω_m) decreases as torque (T_a) increases or vice versa. This relation is expressed by equation (37).

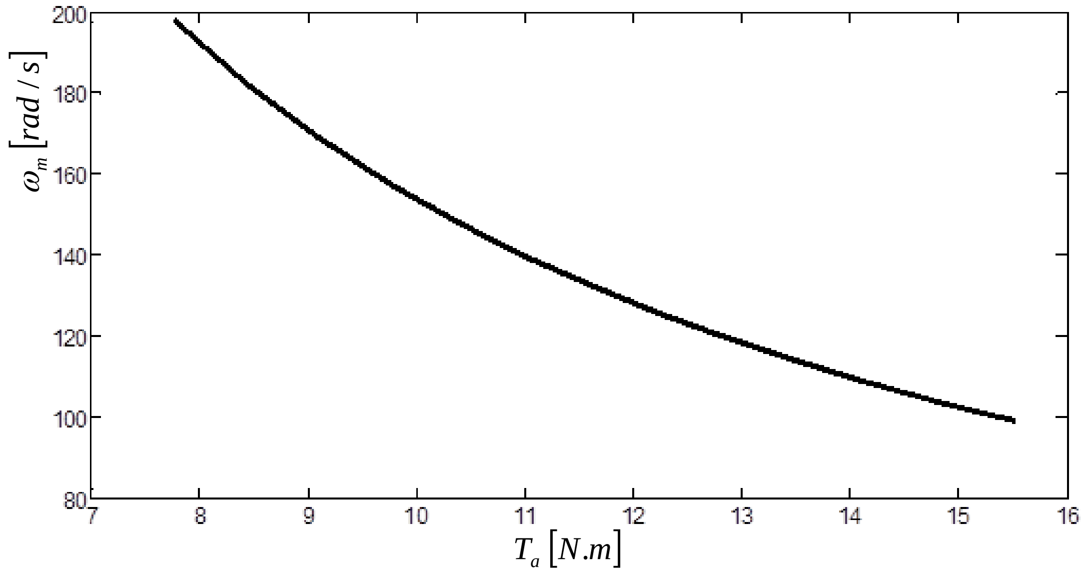

Fig. 15 Plot of Torque Versus Speed.

IV. CONCLUSION

In this thesis the features and operations of different types of dc motor have been presented. The speed of dc motors is controlled by various mean. This thesis has examined speed control of separately excited dc motor by single phase semi-controlled rectifier. This rectifier provides one-quadrant operation, where both the output voltage and current have positive polarity. The principle of operation of the the rectifier has been analized. The output current of the rectifier is continuous by virtue of the free-wheeling diode. It has been shown in this thesis that the armature voltage is varied to obtain a speed up to base speed, while the torque is maintained constant. For the base speed to be exceeded, the field current has to be decreased from the rated value. As the torque requirement is decreased, the speed increases. Closed-loop feedback systems are prevalent in industrial drive systems since they enhance accuracy and fast dynamic response. Therefore, closed-loop control was also investigated in this thesis. The transfer functions, which represent the dynamic behavior of the motor with respect to the two possible inputs (armature voltage and load torque) were obtained. The steady-state responses of the motor were obtained by combining the individual response due to the armature voltage and the load torque. Ultimately, it has been shown that, with both armature voltage control and field voltage control the speed and the torque of the motor can be adjusted.

REFERENCES

Daniel, W. H. (2011). *Power Electronics*, New York: McGraw-Hill.

Sen, P. C. (1995). Electric Motor Drives and Control: past, present and future. *IEEE Transactions on IndustrialElectronics*, 37(6), pp. 562-575

Donnelly, E.L (1972). Electrical Installation Theory and Practice 2nd Edition. London University Press U.K.

Khaled, A. H. S. (2013). Simulation of AC-Dc Converter for DC Motor Application using Fuzzy Logic Control. This project report presented in partial fulfillment of the requirements for the award of the Degree of Master of Electrical Engineering Faculty of Electrical and Electronic Engineering UniversitiTun Hussein Onn, Malaysia.

Morgan,M.(1997).MorganMotorCompany.**Retrievedfrom** https://www.educationindex.com/essay/Case-Study-Morgan-Motor-Company-FKY343SC2Z

Dubey, G. K. (1989). *Power Semiconductor Controlled Drives*. Englewood N.J.: Prentice Hall, pp. 72-75

Onah, A.J., Awah, C.C. and Diyoke, G.C. (2022). Speed Control of Direct Current Motors. *Nigerian Research Journal of Engineering and Environmental Sciences*, 7(1): 319-329.

Malatestas, P, (2013). *Motor Drives.* Tziolas Publications: Athens, Greece, (In Greek).

Rashid, M. H. (1993). *Power Electronics: Circuits, Devices, and Applications*. Prentice Hall Inc., pp. 493-513.

Kazuaki, F. and Hirotaka, K. (2014). Analysis of Half-Wave Class DE Low dv/dt Rectifier at Any Duty Ratio, *IEEETransactions on Power Electronics*, 29(1), pp. 3657-3668

Jha, A. K., Fernandes, B. G. and Kishore, A. (2006). *A Single Phase Single Stage AC/DC Converter with High Input Power Factor and Tight Output Voltage Regulation*. Indian Institute of Technology. India. pp:322-329.

Jomy, J., Edwina, G. R. and Santhosh, R. (2009). A Modified SEPIC Converter Fed Induction Motor Drive. *IOSR Journal of Electrical and Electronics Engineering (IOSR-JEEE). International Conference on Future Technology in Engineering – ICFTE'16.*

.